Portable device integrating an ultrasensitive mechanical crack-based sensor for the wireless monitoring of cardiac activity

Nicolas De Pinho Ferreira
Institut des Nanotechnologies de Lyon
INSA de Lyon
Villeurbanne, France
nicolas.depinhoferreira@insa-lyon.fr

Etienne Puyoo
Institut des Nanotechnologies de Lyon
INSA de Lyon
Villeurbanne, France
etienne.puyoo@insa-lyon.fr

Bertrand Massot
Institut des Nanotechnologies de Lyon
INSA de Lyon
Villeurbanne, France
bertrand.massot@insa-lyon.fr

Solène Brottet
Institut des Nanotechnologies de Lyon
INSA de Lyon
Villeurbanne, France
solene.brottet@insa-lyon.fr

Christophe Malhaire
Institut des Nanotechnologies de Lyon
INSA de Lyon
Villeurbanne, France
christophe.malhaire@insa-lyon.fr

***Abstract*— Flexible crack-based strain sensors showing a maximum gauge factor of 30,000 at 0.2% strain level are elaborated by means of Atomic Layer Deposition and e-beam evaporation. It is shown that the mechanosensitivity can be drastically boosted by encapsulating the cracks with a photoresist layer. A non-invasive portable device integrating this ultrasensitive flexible transducer is then developed to monitor the cardiac activity at rest. The presented prototype integrates a Bluetooth Low Energy wireless interface for real-time communication with an Android mobile device.**

Keywords—Flexible technology, crack-based strain sensor, arterial-pulse sensor, Atomic Layer Deposition.

I. Introduction

Piezoresistive transducers are widely used in the field of flexible/stretchable electronics to develop a variety of applications ranging from robotics to wearable systems and mobile healthcare [1]. During the last decade, the research in the field has mainly been focused on the development of new concepts to optimize sensitivity, power consumption and miniaturization. Among the different approaches that have been proposed in literature these past few years, the technology of crack-based transducers gives rise to the highest gauge factors by far [2]. The concept of crack-based sensors is very straightforward: under mechanical stress, the gradual opening of pre-formed cracks in a conductive thin layer generates a giant variation in its electrical resistance. According to literature [2, 3], the maximum gauge factor and optimal sensing range are directly related to the morphology of the cracks.

In a recent paper [3], we have demonstrated that nanostructured thin films (TF) made of Pt nanoparticles encapsulated in a brittle Al_2O_3 layer can generate cracks with low dispersion and small average asperity height leading to giant gauge factors at low strain levels (<1%). These flexible nanostructured transducers have also been used to monitor the arterial-pulse activity when stuck to the wrist of a person at rest. Here, we are pushing this demonstration forward by further optimizing the crack-based transducer (cost and sensitivity) and by developing a complete portable device communicating with an android application through a wireless interface.

II. Crack-based sensor integration

In this work, our first objective was to lighten the elaboration process by replacing the nanostructured transducer presented in [3] by an Al_2O_3/Ti/Pd stack. The transducer based on Pt nanoparticles had indeed several drawbacks mainly related to its elaboration process by atomic layer deposition. The $MeCpPtMe_3$ precursor that was used for Pt growth is highly expensive (~250 k€/kg), it has a short life span (inferior to three months) and it leads to ultralow growth rates in the range of 10^{-3} nm.s^{-1} [4, 5]. In comparison, Pd is a stable material that can be grown by physical vapor deposition at a much higher rate (>1 nm.s^{-1}) and at a lower cost (~22 k€/kg).

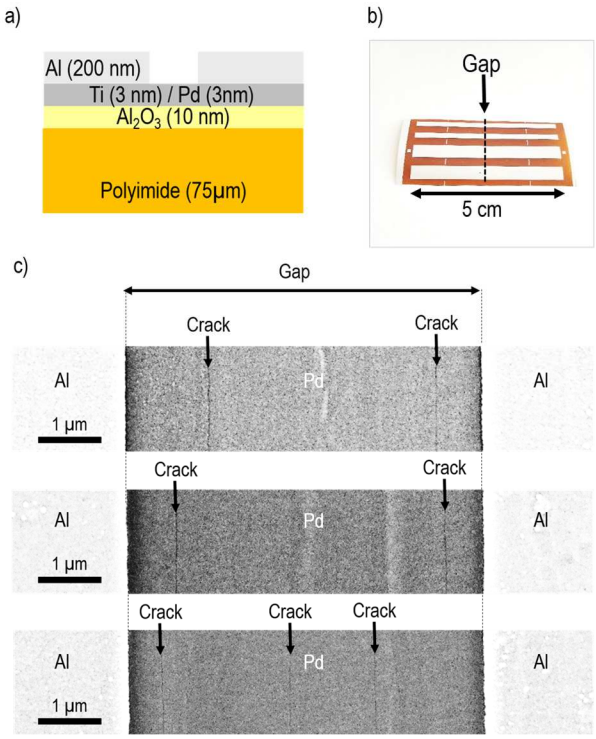

Fig. 1. a) Schematic cross-section and b) photograph of the flexible strain sensor; c) Top view SEM images of a 6µm gap after crack formation.

Figure 1a presents a schematic cross section of an Al_2O_3/Ti/Pd stack integrated on a flexible substrate. A 10 nm thick Al_2O_3 layer is first grown at 200°C by atomic layer deposition using trimethyl-aluminium and water precursors on a 75 µm thick polyimide substrate. After that, a 6 nm thick Ti/Pd bilayer is deposited by e-beam evaporation. The role of the brittle Al_2O_3 thin film is to promote later the crack formation at low strain level (around 1%). Then, 200 nm thick Al top contacts are patterned by a lift-off process combining UV lithography and e-beam evaporation (see the photograph in Fig.1b). A series of gaps ranging from 2 µm to 16 µm are patterned between the Al top electrodes.

To generate the cracks within the TiPd conducting film, the flexible sensor is submitted to a 1% tensile strain level in a buckling configuration. The sample is fixed between two mobile supports; the distance between them is progressively reduced to obtain the buckling state, while measuring the resistance to detect the instant when the first cracks are formed. Figure 1c presents top-view scanning electron microscopy images carried out on a 6 µm-long gap after crack formation. Two or three parallel cracks are clearly visible on each of the three different scanned positions within the gap.

Finite Element Modeling (FEM), using ANSYS® software, was performed to better understand the process of crack formation. In a previous work [6], the calibration curve of a buckled polyimide beam was given and compared with both a simple analytical model and finite element simulations, in which only the polyimide layer was meshed with 3D solid elements (SOLID186). In order to study more precisely the deformation field at the surface of the Al/Pd/Ti/Al_2O_3/Polyimide composite beam, and in particular at the gap between the two Al top electrodes, new FEM simulations are performed using multilayered SHELL281 elements. A non-linear buckling analysis (a small force is applied to pre-bend the beam slightly upwards) is followed by a post-buckling analysis in which a uniform displacement is imposed at each end of the beam. The parameters used in the model are reported in Table I. For a total displacement of 6mm, the longitudinal strain at the surface of the Pd layer (namely at the Al/Pd interface when electrodes are present) is plotted in Fig. 2a as a function of the gap length between the two Al electrodes. As expected, the deformation is maximum where the beam is the thinnest, i.e. at the gap. Compared to the case where the Al film covers the entire surface of the beam (0µm gap), an increase of about 0.15% is observed at the Pd surface at the gap. The formation of one or more cracks is therefore expected logically in this region. The inter-electrodes distance has no significant influence on this increase in deformation. At the contrary, by increasing the thickness of the electrodes, the contrast in stiffness between the gap region and the rest of the beam increases. As shown in Fig. 2b, the elastic strain at the surface of the Pd layer is shifted significantly: almost +0.2% for a 500 nm thick electrode compared to a 200 nm thick one (note that the slopes close to the gap region are due to a poor mesh density).

TABLE I. PARAMETERS USED IN THE FEM SIMULATIONS

Layer	Thickness (nm)	Young's modulus (GPa)	Poisson's ratio	Reference
Al	200 to 500	70	0.33	[7]
Pd	3	121	0.39	[8]
Ti	3	115	0.32	[7]
Al_2O_3	10	165	0.3	[9]
Polyimide	75 000	3.4	0.34	[6]
Beam size: 28 mm × 5 mm				
Gap between the two Al electrodes: 20 µm to 1000 µm				

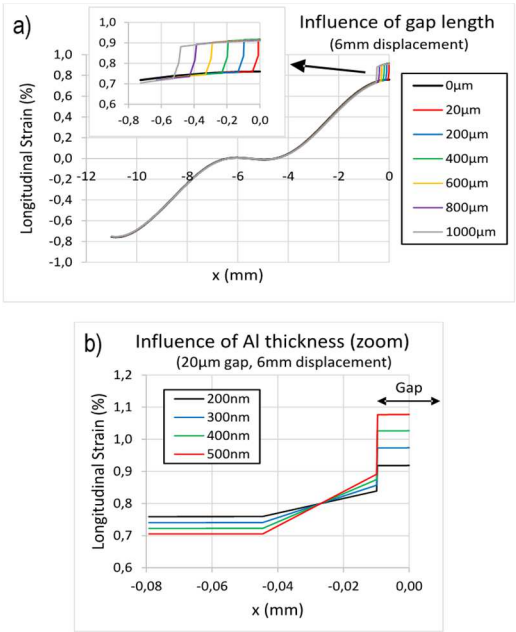

Fig. 2. FEM results that show the influence of the gap length (a) and Al top electrode thickness (b) on the local strain within the gap.

III. ELECTRO-MECHANICAL RESPONSE ANALYSIS

The electro-mechanical response of the flexible sensor is tested in a buckling configuration according to the experimental procedure described in [6]. In order to avoid any

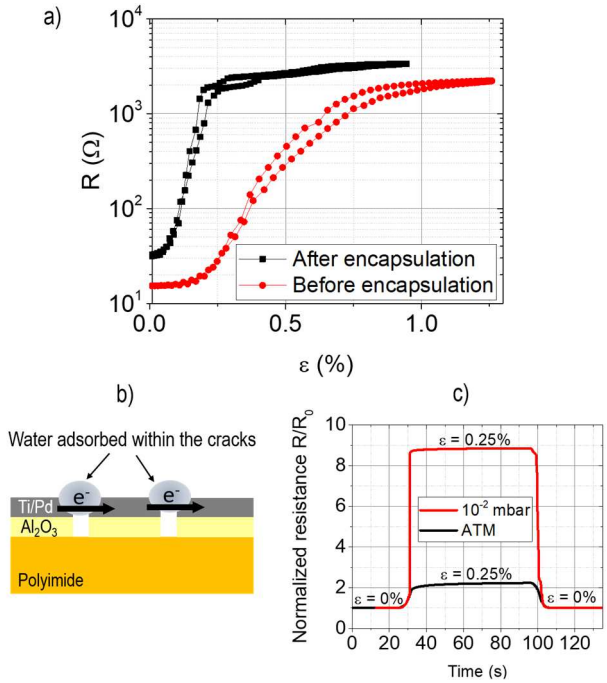

Fig. 3. a) Sensitivity curves obtained before and after encapsulation of the cracks; b) Schematic illustrating the presence of water droplets adsorbed within the cracks; c) Resistance variation of the transducer submitted to a 0.25% strain load in vacuum and in air.

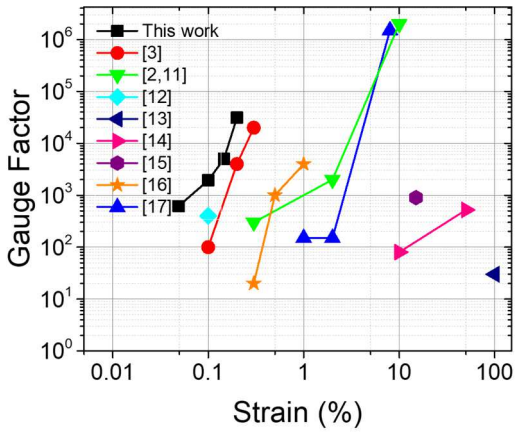

Fig. 4. Comparison of gauge factors obtained by different groups with the crack-based technology.

effect of moisture, the flexible sensor is encapsulated with a 1.1µm thick photoresist layer (AZ5214 from Microchemicals). Prior to encapsulation by spin-coating in air, the substrate is preheated at 120°C during 10 minutes and then coated with an hydrophobic HMDS primer. After spin-coating, the photoresist is annealed at 120°C during 15 minutes in order to evaporate the solvent and some residual water adsorbed on the surface.

The measured electromechanical responses of the cracked sensor before and after encapsulation are compared in Figure 3a. A slight hysteresis is observed on both curves which can be due to adhesion forces between the crack lips and/or to viscoelastic effects within the polyimide substrate. Most importantly, it is shown that the sensitivity can be drastically enhanced at low strain level by encapsulating the cracked TiPd film with a photoresist. We believe that the photoresist is possibly submitted to an internal compressive stress that shifts the sensitivity curve to low strain levels. Another possible explanation might be related to the influence of humidity on the electrical resistance of the cracks.

In reference [10], Hong et al. have shown that some water droplets can be adsorbed within the cracks to form current paths under high humidity level (figure 3b). This water adsorption leads to a decrease of the strain sensor resistance. Under high humidity, a high strain level would therefore be necessary to break these water conducting paths in order to reach the high resistance state of open cracks. In figure 3c, we compare the normalized resistance variations of the nonencapsulated transducer submitted to a 0.25% tensile strain load in vacuum (10^{-2} mbar) and at atmospheric pressure in air. The resistance variation acquired in vacuum is four times higher than in air which means that a higher strain level is necessary in air to reach the high resistance state of electrically opened cracks. This observation seems to confirm that moisture can drastically affect the electro-mechanical response of the crack-based transducer. As shown in [10], shielding the cracks by encapsulation is a way to avoid the influence of humidity.

From figure 3a, a maximum gauge factor of 30,000 can be extracted at a strain level of 0.2%. It should also be noted that the encapsulation of the cracks increases the sensitivity to the detriment of the dynamic range. The encapsulated

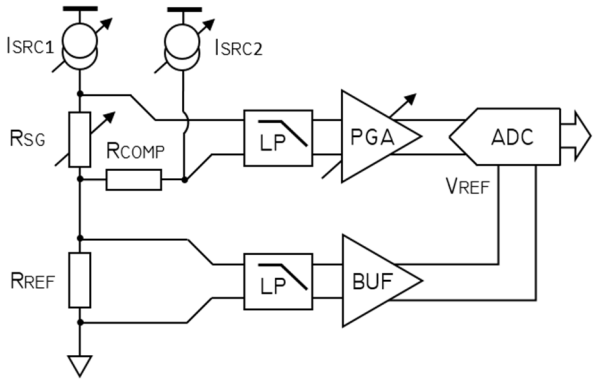

Fig. 5. 3-wire ratiometric circuit for the measurement of the sensor's resistance value.

transducer has indeed a dynamic range from only 0.05% to 0.25% strain levels whereas the bare cracked-sensor can operate from 0.2% to 1% strain. As compared to other groups working on the technology of crack-based transducers (figure 4), this giant gauge factor of 30,000 is, to the best of our knowledge, at the state of the art [2,3,11-17]. We also emphasize the fact that the encapsulated Al_2O_3/Ti/Pd stack shows a greater sensitivity than the nanostructured transducer presented in our previous study [3].

IV. Development of the Portable Device

Measurement of the sensor's resistance is achieved by using a 3-wire ratiometric circuit (Fig. 5). This type of circuit topology is commonly used for precise resistance measurement, for example resistance temperature detector (RTD) sensors, and thus was adapted in our application to the crack-based sensor. For this purpose, the ADS1247 (Texas Instrument) integrated circuit was used. This component offers two programmable current sources as well as a 24 bits, 2 ksps delta-sigma analog to digital converter (ADC). Here, the ratiometric measurement topology improves the overall system noise performance as the same current is shared by both the sensing element (R_{SG}), and the resistance R_{REF} which is used to adjust the ADC reference voltage (Eq. 1). The R_{COMP} resistor is used to set the middle point of the differential voltage developed across inputs of the programmable gain amplifier (PGA) and thus, ADC (Eq. 2). If the value for R_{COMP} is selected in the order of magnitude of R_0 (steady resistance of the sensing element), the resulting differential voltage is directly proportional to the variation of the sensor resistance ΔR, when both current sources deliver an identical current I (Eq. 3). The injected current level is maintained below 500 µA in order to prevent any self-heating effect on the strain gauge. Two differential low-pass filters with cut-off frequencies of 25 Hz provide attenuation for both differential and common mode noise signals.

$$V_{REF} = 2I \cdot R_{REF} \quad (1)$$

$$V_{PGA} = I_1(R_0 + \Delta R) - I_2 \cdot R_{COMP} \quad (2)$$

$$V_{ADC} = G_{PGA} \cdot I \cdot \Delta R \quad (3)$$

with G_{PGA} = 256 V/V, I = 250 µA and the strain gauge peak-to-peak resistance variation $|\Delta R| \cong 15\ \Omega$ the differential

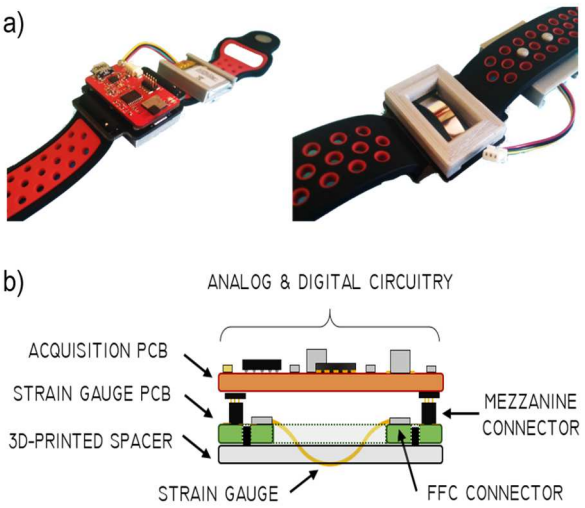

Fig. 6. a) Top-view of the embedded electronic board and bottom view of the sensor in buckling configuration with 3D-printed support; b) mechanical integration of the sensor and assembly with electronic board.

voltage present at ADC inputs is approximatively 0.96 V. Meanwhile, the ADC reference voltage is 1.65 V with R_{REF} = 3.3 kΩ. Experimental parameters such as pre-strain (applied by wristband attaches) or strain gauge deformation caused by radial artery is likely to vary among the different users of the device. To maintain the analog front end in its optimal operating point, injected current and PGA gain can be remotely adjusted.

Data sampled by the ADS1247 are collected using a serial peripheral interface (SPI) bus and sent wirelessly by a microcontroller unit (MCU) which integrates a Bluetooth Low Energy (BLE) transceiver and its associated software stack. The MCU used in the circuit (BGM13S, SiliconLabs) also offers the advantage to integrate a 2.4 GHz antenna so that space is saved on the overall printed circuit board. We developed a custom firmware on the MCU to enable the configuration of data acquisition wirelessly through the BLE communication. Additionally, a LiPo battery circuit management was designed to charge an embedded battery when the system is connected to a USB charger or to a USB port on a computer using a micro-B USB connector. Figure 6a illustrates the electronic embedded system attached on a wristband with a 150 mAh embedded LiPo battery.

The flexible sensor is mounted on a separated PCB which can be stacked to the main circuit board by using mezzanine connectors. The sensor itself is attached on this PCB with flat flexible cable (FFC) whose width matches the size of the sensor (figure 6b). The length of the two Al top electrodes on the sensor can be adjusted to put the sensor in a buckling configuration, so a pre-stressing is applied on the strain sensor to set the operating point (figure 6). A 3D-printed support is appended to the sensor PCB to maintain a constant height between the skin and the circuit and thus leave the sensor closed to the operating point when applied on to the skin (figure 6).

A custom Android application was developed to connect to the microcontroller unit and thus collect data sent from the sensor. The interface enables to adjust circuit parameters such as current source values, gain and sample rate (from 5 up to

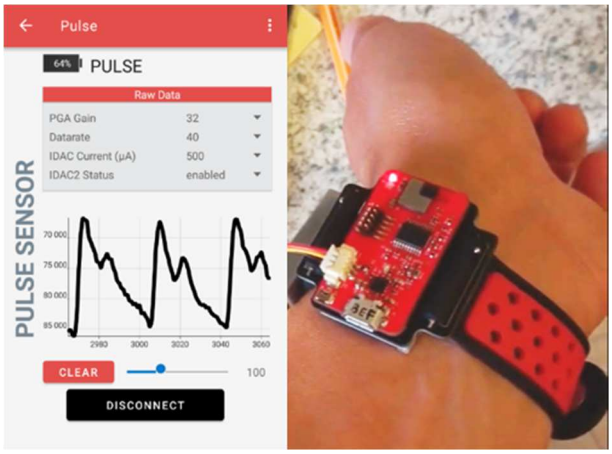

Fig. 8. Screenshot of the PulseSensor Android application and photograph of the portable device mounted on a wrist.

160 samples per second). Figure 7 shows the application running on an Android smartphone connected to the portable device and the signal waveform obtained from the sensor. Data are recorded on a CSV text file on the smartphone and can then be retrieved to be processed on a computer. As shown in our previous study [3], a heart rate in bpm and some physiological information (detection of percussion and tidal waves, respiratory activity) can be extracted from the arterial-pulse activity signal. It should also be noted that two complete portable devices mounted last summer (August 2019) are still working today (June 2020) which means that our system has a life span of at least a tenth of months.

V. Conclusion

In summary, we have integrated cracked Al_2O_3/Ti/Pd stacks on flexible substrate at low temperature in order to develop ultrahigh sensitive strain sensors. From FEM simulations, we could first demonstrate that the thickness of the Al top electrodes clearly modifies the local strain while the size of the gap between them has no influence on the deformation level. A giant gauge factor of 30,000 could be obtained at 0.2% strain level thanks to the encapsulation of the cracks with a photoresist layer. This optimized crack-based transducer was finally integrated on a home-made portable device that successfully demonstrated wireless communication with an Android mobile device and feasibility of arterial-pulse activity monitoring.

Acknowledgment

This work has been founded by a Bonus Quality Research (BQR) program from INL. The authors would like to thank Joëlle Grégoire for her technical support on the NanoLyon technological platform.

References

[1] M. Amjadi, K.-U. Kyung, I. Park and M. Setti, “Stretchable, skin-mountable, and wearable strain sensors and their potential applications: a review,” Adv. Funct. Mater., vol 26, pp. 1678-1698, 2016.

[2] D. Kang, P. V. Pikhitsa, Y. W. Choi, C. Lee, S. S. Shin, L. Piao, B. Park, K.-Y. Suh, T.-i. Kim and M. Choi, “Ultrasensitive mechanical crack-based sensor inspired by the spider sensory system,” Nature, vol. 516, pp. 222-226, 2014.

[3] E. Puyoo, S. Brottet, R. Rafaël and C. Malhaire, "Ultrahigh sensitivity to strain of cracked thin films based on metallic nanoparticles in a dielectric matrix," IEEE Sensors Letters, vol. 2(3), pp.1-4, 2018.

[4] L. Baker, A. S. Cavanagh, D. Seghete, S. M. George, A. J. M. Mackus, W. M. M. Kessels, Z. Y. Liu and F. T. Wagner, "Nucleation and growth of Pt atomic layer deposition on Al2O3 substrates using (methylcyclopentadienyl)-trimethyl platinum and O2 plasma," Journal of Applied Physics, vol. 109, pp. 08433, 2011.

[5] D. Thomas, E. Puyoo, M. Le Berre, L. Militaru, S. Koneti, A. Malchère, T. Epicier, L. Roiban, D. Albertini, A. Sabac and F. Calmon, "Investigation of the in-plane and out-of-plane electrical properties of metallic nanoparticles in dielectric matrix thin films elaborated by atomic layer deposition," Nanotechnology, vol. 28, pp. 455602, 2017.

[6] E. Puyoo, C. Malhaire, D. Thomas, R. Rafael, M. R'Mili, A. Malchère, L. Roiban, S. Koneti, M. Bugnet, A. Sabac and M. Le Berre, "Metallic nanoparticle-based strain sensors elaborated by atomic layer deposition," Applied Physics Letters, vol. 110, pp. 123103, 2017.

[7] M. Chinmulgund, R.B. Inturi and J.A. Barnard, "Effect of Ar gas pressure on growth, structure, and mechanical properties of sputtered Ti, Al, TiAl, and Ti_3Al films," Thin Solid Films, vol. 270, pp. 260-263, 1995.

[8] S.U. Jen and T. C. Wu, "Young's modulus and hardness of Pd thin films," Thin Solid Films, vol. 492, pp. 166-172, 2005.

[9] Maria Berdova, "Micromechanical characterization of ALD thin films," Doctoral dissertations 119/2015, 80 p. Aalto University publication series, ISBN 978-952-60-6345-4.

[10] S. K. Hong, S. Yang, S. J. Cho, H. Jeon and G. Lim, "Development of waterproof crack-based stretchable strain sensor based on PDMS shielding," Sensors, vol. 18, pp. 1171, 2018.

[11] Y. W. Choi, D. Kang, P. V. Pikhitsa, T. Lee, S. M. Kim, G. Lee, D. Tahk and M. Choi, "Ultra-sensitive pressure sensor based on guided straight mechanical cracks," Scientific Reports, vol. 7, pp. 40116, 2017.

[12] F. Liao, C. Lu, G. Yao, Z. Yan, M. Gao, T. Pan, Y. Zhang, X. Feng and Y. Lin, "Ultrasensitive flexible temperature-mechanical-dual-parameter sensor based on vanadium dioxide films," IEEE Electron Device Letters, vol. 38(8), pp. 1128-1131, 2017.

[13] C.-J. Lee, K. H. Park, C. J. Han, M. S. Oh, B. You, Y.-S. Kim and J.-W. Kim, Scientific Reports, vol. 7, pp. 7959, 2017.

[14] M. Amjadi, M. Turan, C. P. Clementson and M. Sitti, "Parallel microcracks-based ultrasensitive and highly stretchable strain sensors," ACS Appl. Mater. Interfaces, vol. 8, pp. 5618-5626, 2016.

[15] Y. Jiang, Z. Liu, N. Matsuhisa, D. Qi, W. R. Leow, H. Yang, J. Yu, G. Chen, Y. Liu, C. Wan, Z. Liu and X. Chen, "Auxetic mechanical metamaterials to enhance sensitivity of stretchable strain sensors," Adv. Mater., vol. 30, pp. 1706589, 2018.

[16] S. Chen, Y. Wei, S Wei, Y. Lin and L.Liu, "Ultrasensitive cracking-assisted strain sensors based on silver nanowires/graphene hybrid particles," ACS Appl. Mater. Interfaces, vol. 8(38), pp. 25563-25570 , 2016.

[17] J. Tolvanen, J. Hannu and H. Jantunen, "Stretchable and washable strain sensor based on cracking structure for human motio monitoring," Scientific Reports, vol. 8, pp. 13241, 2018.